Penning Ionization of NCCN by Experiment and Theory: A Two-Dimensional Penning Ionization Electron Spectroscopic and Quantum Chemical Study

Tibor Pasinszki,*,† Naoki Kishimoto, Tetsuji Ogawa, and Koichi Ohno*

Department of Chemistry, Graduate School of Science, Tohoku University, Aramaki, Aoba-ku, Sendai, 980-8578, Japan

Received: March 26, 1999; In Final Form: June 10, 1999

Dicyanogen, NCCN, is generated for spectroscopic investigations on-line from rubeanic acid, mercury(II) cyanide, and cyanogen iodide and studied in the gas phase by two-dimensional Penning and He I photoelectron spectroscopies, as well as ab initio calculations. From spectroscopic data, the interaction between NCCN and He*(2^3S) atoms is deduced. The interaction potential for the similarly interacting NCCN−Li(2^2S) system is obtained from ab initio calculations at the CCSD/6-311++G** level. Experimental and calculated results show that the interaction potential is anisotropic around NCCN, is the most attractive in the nitrogen lone electron pair region, and gradually changes into repulsive as the N−C−He*(or Li) angle opens up to 90°. An unusual collision energy dependences of the partial ionization cross sections are observed, which is interpreted by the unusual interaction potential. For assisting experimental data and studying collision dynamics, classical trajectory calculations are performed for the Penning ionization of the NCCN−He*(2^3S) system. The spectroscopic investigations predict the existence of thermodynamically stable MLi radicals, and the structure and stability of NCCNLi isomers are calculated at the QCISD/6-311++G** level.

I. Introduction

When a He*(2^3S) metastable atom, having much higher excitation energy than the ionization potential (IP) of the molecule, collides with a molecular target (M), ionization may occur, which yields the ground-state helium atom (He), molecular positive ion in a given electronic state (M_i^+), and a free electron (e^-):[1]

$$He^* + M \rightarrow He + M_i^+ + e^- \quad (1)$$

The ionization process may be divided into three parts: (I) the approach of the metastable atom to the molecule; (II) ionization; (III) relaxation of the excited-state positive ion and secondary ionic reactions. In Penning ionization electron spectroscopy (PIES), the electron ejected in this process is analyzed. The PIES spectrum, therefore, provides primary information about the state of the system in the "moment" of ionization and secondary information about what happened before that. In particular, the kinetic energy and number of electrons, which determines the peak positions and relative branching ratios in the spectrum, provides information about the electronic structure of the molecule, the relative ionization probability of different ionic states, and the potential energy difference between the incoming M + He*(2^3S) and outgoing M_i^+ + He systems at the geometry of ionization (II). By measuring the electron intensity, compared to that of metastable atoms in the incident metastable beam, the total and partial ionization cross section (σ) can be determined. This latter, however, may depend on what happens if molecules and metastable atoms get into close interaction (I); attractive interaction is expected to increase the ionization cross section by increasing the number of trajectories leading to ionization, and repulsive interactions to decrease it.

Two-dimensional Penning ionization electron spectroscopy (2D-PIES) has been recently developed in our laboratory,[2] in which ionization cross sections are determined as a function of both electron kinetic energy and metastable atom collision energy. The method, is thus ionic state and collision energy resolved, and makes it possible to study the collision energy dependence of the total and partial ionization cross sections and to derive information about the interaction between molecules and metastable atoms. One-dimensional cuts from the two-dimensional spectrum give the collision energy dependence of partial ionization cross sections (CEDPICS; ionic state is fixed) and collision energy resolved PIES (CERPIES; metastable atom kinetic energy is constant). Since an ionic state originates from removing an electron from a molecular orbital (MO), the dependence of the partial ionization cross section reflects the interaction in the molecular region where the MO is localized; therefore, it is possible to study the interaction between structural elements of the molecule (e.g., chemical groups, chemical bonds, electron lone pairs) and metastable atoms. Since there is a well-known similarity between M + He*(2^3S) and M + Li(2^2S) interaction potentials, and given that this latter is the ground state potential of the M−Li system, indirect information can be obtained about this latter chemically important interaction too.[3] We have recently successfully applied 2D-PIES to study the anisotropy of the interaction potential between He*(2^3S) atoms and alcohols, thioalcohols, thioethers, and nitriles.[4,5]

Although 2D-PIES is proved to be a powerful technique to study the Penning ionization, interaction potential, and collision dynamics of the interacting M + He*(2^3S) system, it is rather limited regarding this latter one. To get a deeper insight into the collision dynamics and also to assist in analyzing experimental data on a theoretical basis, we have recently developed a novel theoretical method (see discussion section) to calculate ionization cross section and collision energy dependence of the total and partial Penning ionization cross sections.[6] As the first

* Corresponding author. E-mail: ohnok@qpcrkk.chem.tohoku.ac.jp.
† Permanent address: Department of Inorganic Chemistry, Technical University, H-1521 Budapest, Hungary.

10.1021/jp991049y CCC: $18.00
Published on Web 08/21/1999

SCHEME 1

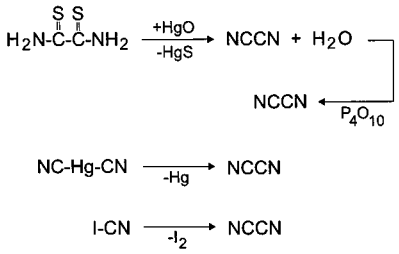

example, we applied this method to study the Penning ionization of nitrogen ($He^*(2^3S) + N_2 \rightarrow He + N_2^+ + e^-$),[6] and the complete success of describing the collision energy dependence of the total and partial ionization cross sections prompted us for further testing. Nitrogen itself is a simple molecule with high symmetry and, although the interaction potential is anisotropic, it represents the case where the interaction is repulsive with $He^*(2^3S)$ atoms at any collision direction. It was thus self-evident that we wanted to test the performance of our method on a system where the interaction is attractive. Our previous study on various nitriles (R−CN) indicated that the interaction potential with $He^*(2^3S)$ is attractive around the −CN group, especially in the nitrogen lone electron pair region.[3,5] Putting two of these groups together, the parent pseudohalogen NCCN seemed to be the desired target. As it turns out from this work, however, the ionization of NCCN has a very unusual collision energy dependence in the investigated collision energy region, and we might have unknowingly selected one of the most difficult targets to describe. Another aim, to study NCCN by 2D-PIES, came from our previous work on substituted nitriles,[3,5] where a very strong attractive interaction was observed in the nitrogen lone pair region, and to find out substituent effects, the study of the parent pseudohalogen seemed to be essential. Simple pseudohalides seem to have an interesting and varied electronic structure. Our current PIES and ab initio study on pseudohalo acids (HCNO, HNNN, HNCO, HNCS)[7] showed that these molecules form thermodynamically stable four-membered ring π-complexes with lithium atoms, where the lithium 2s unpaired electron is delocalized on the acid. To investigate the complex formation of Li with NCCN as an entrée for our future investigation on gaseous $Li_n(NCCN)_m$ clusters was another initiative of this work.

In this paper, we present a combined experimental and theoretical study of the interaction of NCCN with $He^*(2^3S)$ and Li atoms using 2D-PIES and ab initio calculations. Relevant to this work are the earlier photoelectron spectroscopic investigations[8−11] and the early PIES investigations using a mixture of singlet and triplet metastable atoms, $He^*(2^1S,2^3S)$.[12,13] Of particular interest are the electronic structure, the anisotropy of the interaction between NCCN and $He^*(2^3S)$ or $Li(2^2S)$ atoms, and the collision dynamics, as well as the possible existence, stability, and structure of M−Li inorganic radicals.

II. Experimental Section

Generation of NCCN. NCCN has been known for a long time and has become an important reagent in laboratories and industry. However, it is very toxic and its handling, transportation, and storage requires special conditions. To get rid of these difficulties, we thought it best to generate this gas on-line for spectroscopic investigations. We considered three routes, from rubeanic acid, mercury(II) cyanide (Nacalai tesque), or cyanogen iodide (Aldrich), as discussed below and shown in Scheme 1.

It was observed recently that $CH_3OC(S)NH_2$ vapors reacted fast with yellow mercuric oxide (HgO) at room temperature, and this solid−gas reaction quantitatively produced CH_3OCN and H_2O.[14] In a similar manner, we expected that NCCN could be generated from rubeanic acid ($H_2NC(S)C(S)NH_2$) by two-fold H_2S elimination. A mixture of rubeanic acid and HgO was placed into a horizontal tube, which was attached to another horizontal tube filled at the bottom with P_4O_{10} to catch side product water. The tubes were then connected via a U-trap directly to the spectrometer, and the mixture was heated. By increasing the temperature, the yield for NCCN gradually increased, and at 80 °C the pressure was sufficient for UPS and PIES investigations. Only a small amount of CO_2, NH_3, and unvolatile dark-red solid (believed to be the well-known reaction product of ammonia and NCCN; see ref 15) side products were detected, whose relative amount gradually increased by increasing the temperature. NH_3 could be completely removed from the gas phase by cooling the U-trap down to −30 °C. The raw volatile reaction products were introduced directly into the spectrometer and the UPS spectrum obtained is shown in Figure 1. Pure NCCN was obtained by collecting the gaseous reactions products in a second U-trap with liquid nitrogen, pumping off the more volatile CO_2 at low temperature, and reevaporizing NCCN. The PIES spectrum shown in Figure 1 is obtained by this method.

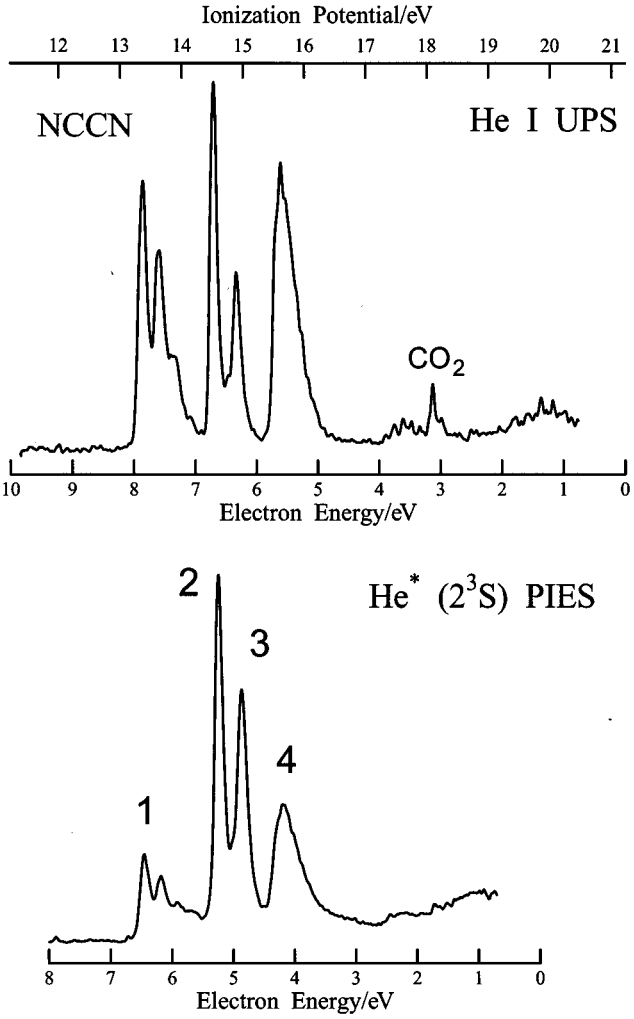

Figure 1. He I UPS and $He^*(2^3S)$ PIES spectrum of NCCN.

The thermal decomposition of $Hg(CN)_2$ to NCCN has been well-known for a long time, and indeed the thermal decomposition of the solid substance led to the discovery of NCCN in 1815 by Gay-Lussac.[16] The thermolysis in this work was carried out as follows. The solid $Hg(CN)_2$ was placed into a one end

blinded Pyrex tube (i.d. 12 mm; loosely packed with quartz wool) and the tube was slowly pulled through a furnace heated to 500 °C. The volatiles of this reaction were collected in a U-trap with liquid nitrogen, and then the temperature was raised to produce enough vapor pressure for NCCN for spectroscopic investigations.

Solid ICN, when it is heated in a closed tube, is known to decompose to NCCN and iodine for some time,[17] and it has sufficient vapor pressure to be easily driven through a furnace in the gas phase under very well-controlled conditions. We carried out the thermolysis in a quartz tube (12 mm i.d.) loosely packed with quartz wool and heated along 25 cm at 800 °C. The furnace was directly connected to the spectrometer via two consecutive U-traps. The temperature of the first trap was held around −60 °C to trap iodine, and NCCN was collected in the second trap.

Spectroscopic Investigations. The instrument used in this work for recording the UPS, PIES, and 2D-PIES spectra was reported in previous papers.[2,18−20] UPS spectra were measured by utilizing the He I resonance line (21.22 eV) produced by a pure helium discharge. Metastable atoms for PIES were produced by a negative discharge nozzle source, and the He*-(2^1S) component of the He*(2^1S,2^3S) beam was quenched by a water-cooled helium discharge lamp. The kinetic energies of electrons ejected by photo or Penning ionization were determined by a hemispherical electrostatic deflection type analyzer using an electron collection angle of 90° to the incident photon or He*(2^3S) beam axis. The energy resolution of the electron analyzer was 50 meV, estimated from the full width at half-maximum (fwhm) of the $Ar^+(^2P_{3/2})$ peak in the He I UPS spectrum. The transmission of the electron energy analyzer was determined by comparing our UPS data of O_2, CO, N_2, and some hydrocarbons with those of Gardner and Samson[21] and Kimura et al.[22]

In the collision energy resolved experiments, 2D-PIES, the metastable atom beam was pulsed by a pseudorandom chopper and introduced into the reaction cell located 504 mm downstream from the chopper disk. As reference, the intensity of metastable atoms were determined by inserting a stainless steel plate into the reaction cell and measuring the intensity of secondary electrons emitted. Thus, in these experiments, the intensity of emitted electrons from sample molecules (I_e) or from a reference stainless steel plate (I_{He*}) were measured as functions of electron kinetic energy (E_{ek}) and time (τ). Electron energies were scanned by 10 meV steps, and a dwell time for the time-dependent measurement was 3 μs. The 2D electron intensity spectra, $I(E_{ek},\tau)$, were then converted sequentially to $I(E_{ek},\tau_{TOF})$ and $I(E_{ek},\nu_{He*})$ (where τ_{TOF} is the time-of-flight and ν_{He*} is the velocity of the metastable atoms). The 2D Penning ionization cross sections $\sigma(E_{ek},\nu_r)$ were obtained from $I(E_{ek},\nu_{He*})$ using eqs 2 and 3, and finally $\sigma(E_{ek},\nu_r)$ was converted to the 2D-PIES, $\sigma(E_{ek},E_c)$ using eq 4:

$$\sigma(E_{ek},\upsilon_r) = c[I_e(E_{ek},\nu_{He*})/I_{He*}(\nu_{He*})](\nu_{He*}/\nu_r) \qquad (2)$$

$$\upsilon_r = [\upsilon_{He*}{}^2 + 3kT/M]^{1/2} \qquad (3)$$

$$E_c = \mu\upsilon_r^2/2 \qquad (4)$$

where c, υ_r, k, T, M, and μ are a constant, the relative velocity of metastable atoms averaged over the velocity of the target molecule, the Boltzmann constant, the gas temperature, the mass of the target molecule, and the reduced mass of the system, respectively.

III. Calculations

The details of the trajectory calculations are given below in the Discussion section. The interaction potential between target molecules (M) and metastable He*(2^3S) atoms were calculated by approximating the M−He*(2^3S) surfaces with those of M−Li(2^2S). Using this widely accepted approximation, based, e.g., on cross-scattering experiments indicating very similar shape for the velocity dependence of the total scattering cross section and for the location and depth of the well of the attractive interaction potential for He*(2^3S) and Li(2^2S) with various atomic and molecular targets,[23,24] all of the difficulties could be bypassed that would be associated with calculating the excited state M−He* surfaces. Thus, the NCCN−Li(2^2S) interaction potentials, $V^*(R,\theta)$ (where R is the distance from the center of mass (X) of the molecule, and θ is the Li−X−N angle), were calculated by pulling the Li atom toward the center of mass of the molecule and keeping the molecular geometry fixed at the experimental values determined from infrared spectroscopic data;[25] this latter assumption meant that the geometry relaxation by the approach of the metastable atom was negligible in the ionization process. All calculations for the interaction potential were done at the CCSD(fc)/6-311++G** level of theory and the full counterpoise (CP) method[26] was used to correct for the basis set superposition errors (BSSE).

The structure of NCCNLi inorganic radicals were fully optimized at the QCISD(fc)/6-311++G** level of theory, and then harmonic vibrational frequencies were calculated at the equilibrium geometries using numeric second derivatives to make sure they were real minima on the potential energy surface. Dipole moments and total atomic charges were calculated using the QCISD density and the natural population analysis. All calculations were performed with the Gaussian-94 quantum chemistry package[27] implemented on Silicon Graphics Inc. Challenge/XL and Origin200 workstations.

The ionization potentials for NCCN were calculated using the outer valence Green's function (OVGF) method[28] as incorporated in Gaussian-94 and also with the semiempirical HAM/3 (hydrogenic atoms in molecules) method,[29] which was shown to give an accurate representation of IPs for molecules containing first-row atoms.[30] OVGF and HAM/3 calculations were performed at the experimental geometry of NCCN.

IV. Results

Figure 1 shows the He I UPS and He*(2^3S) PIES spectrum of NCCN. The electron energy scale for the PIES spectrum is shifted relative to that of UPS by the difference in the excitation energies; 21.22 − 19.82 = 1.40 eV. NCCN is obtained via the rubeanic acid route (see below). The UPS spectrum shows the volatile reaction products; bands of the sideproduct CO_2 are marked. The PIES spectrum is obtained by condensing the reaction products with liquid nitrogen, pumping off CO_2, and then reevaporizing the pure NCCN.

Figure 2 shows a representation of the 2D-PIES spectrum of NCCN. Curves (CERPIES spectra) are obtained from the 2D-PIES spectrum by cutting small kinetic energy regions corresponding to ca. 10 μs TOF of He*. NCCN is generated from ICN for 2D-PIES investigation.

Figure 3 shows the log σ vs log E_c plots of CEDPICS for NCCN (thick lines; between 100 and 300 meV collision energy). The CEDPICS are obtained from the 2D-PIES spectrum by cutting an appropriate range of electron kinetic energy, E_e (typically the fwhm of the corresponding PIES band). The figure also shows the calculated collision energy dependence of the ionization cross sections (thin lines; between 80 and 500 meV

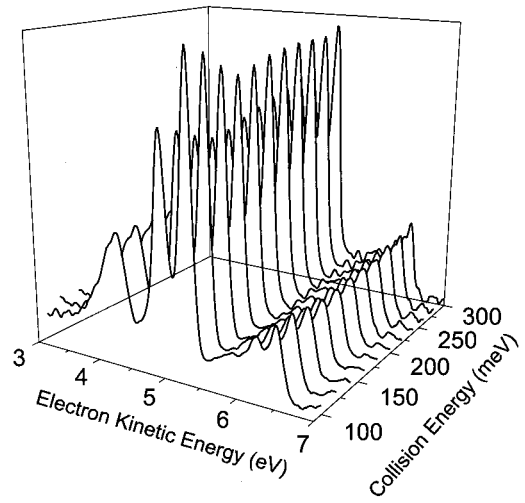

Figure 2. Representation of the 2D-PIES spectrum of NCCN. Curves (CERPIES spectra) are obtained from the 2D-PIES spectrum by cutting small kinetic energy regions.

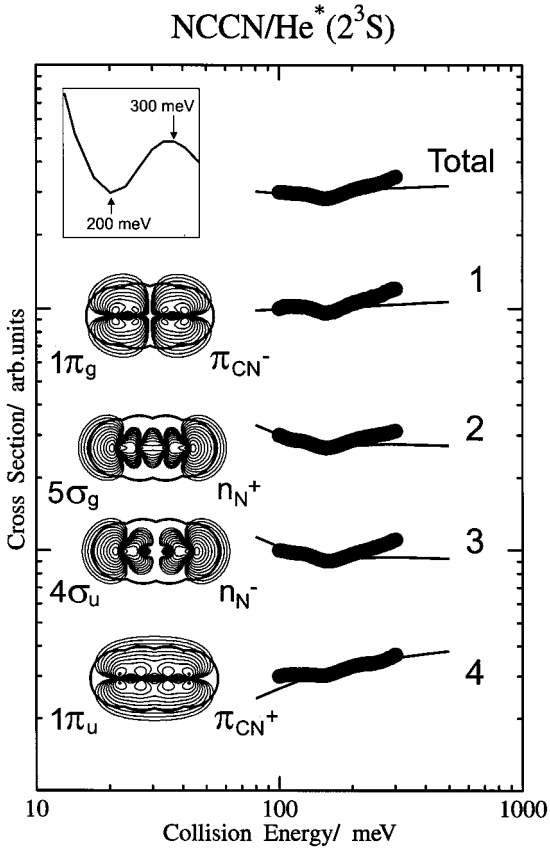

Figure 3. Collision energy dependence of total and partial ionization cross sections for NCCN with He*(2^3S). Thick lines shows experimental data between 100 and 300 meV collision energy, and thin lines indicate calculated values between 80 and 500 meV. Inset in figure shows the calculated collision energy dependence of the ionization cross section for state $B^2\Sigma_u^+$ (number 3) on an expanded scale between 150 and 350 meV collision energy.

collision energy). The calculated electron density maps of the molecular orbitals are also shown in the figure (the thick solid curve in the maps indicates the molecular surface, estimated from the van der Waals radii of atoms). Inset in Figure 3 shows the calculated collision energy dependence of the ionization cross section for state $B^2\Sigma_u^+$ (number 3) on an expanded scale between 150 and 350 meV collision energy.

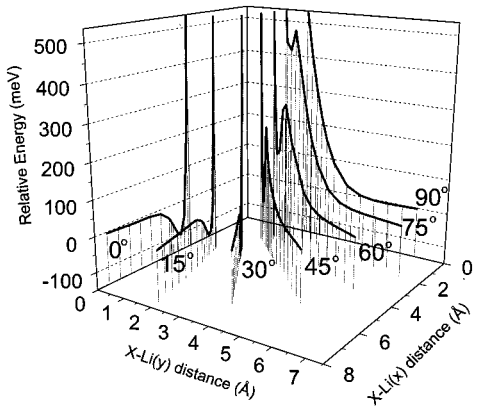

Figure 4. Calculated interaction potential curves between NCCN and Li(2^2S). The origin of the coordinate system is the center of mass (X) of the molecule and NCCN is lying on the x axis. The Li-X−N angle is indicated for each curve.

Figure 4 shows calculated potential energy curves between a ground state Li atom and NCCN. The origin of the coordinate system is the center of mass (X) of the molecule, and NCCN is lying on the x axis. The Li−X−N angle is indicated for each curve. Calculations are done at the CCSD/6-311++G** level of theory.

Figure 5 shows calculated total and partial ionization probabilities for the He*(2^3S)−NCCN chemiionization reaction as a function of the impact parameter b (opacity functions) at collision energy of 200 meV.

Figure 6 shows the calculated equilibrium geometry of LiNCCN inorganic radicals, as well as total atomic charges from natural population analysis using the QCISD density. Calculations were done at the QCISD/6-311++G** level of theory. Bond lengths are given in angstroms.

Table 1 lists experimental and calculated ionization potentials (IPs), experimental peak energy shifts (ΔE), slope parameters (m_1 and m_2) of log σ vs log E_c plots (see text), and the assignment of the spectra. Vertical IPs are determined from the He I UPS spectrum. The peak energy shifts in PIES spectrum are obtained as the difference between the peak position (E_{PIES}; electron energy scale) and the "nominal" value (E_0 = difference between the metastable excitation energy and target IP): $\Delta E = E_{PIES} - E_0$. Table 2 lists the calculated harmonic vibrational frequencies, infrared intensities, rotational constants, dipole moments, and energies of LiNCCN radicals.

V. Discussion

PIES Investigations and the Interaction Potential. NCCN is a high-symmetry linear molecule with a ground state configuration of

$$... (3\sigma_g)^2(3\sigma_u)^2(4\sigma_g)^2(1\pi_u)^4(4\sigma_u)^2(5\sigma_g)^2(1\pi_g)^4; \quad {}^1\Sigma_g^+$$

The observed UPS and PIES spectrum corresponds to four ionic states with the sequence $X^2\Pi_g$, $A^2\Sigma_g^+$, $B^2\Sigma_u^+$, and $C^2\Pi_u$. On the basis of previous UPS investigations[8−11] and theoretical works,[31−34] which discussed assignment and correlation effect on ionization potentials in detail, the discussion of the assignment of the spectra is not necessary (see Table 1). We discuss, however, briefly the shape or localization of MOs, because the information derived on the interaction potential depends on that. Molecular orbital density plots are shown in Figure 3. We note that the calculated pole strengths for ionizations are close to 1, thus the molecular orbital model for ionization of NCCN in the investigated IP region is in order. The first and fourth band

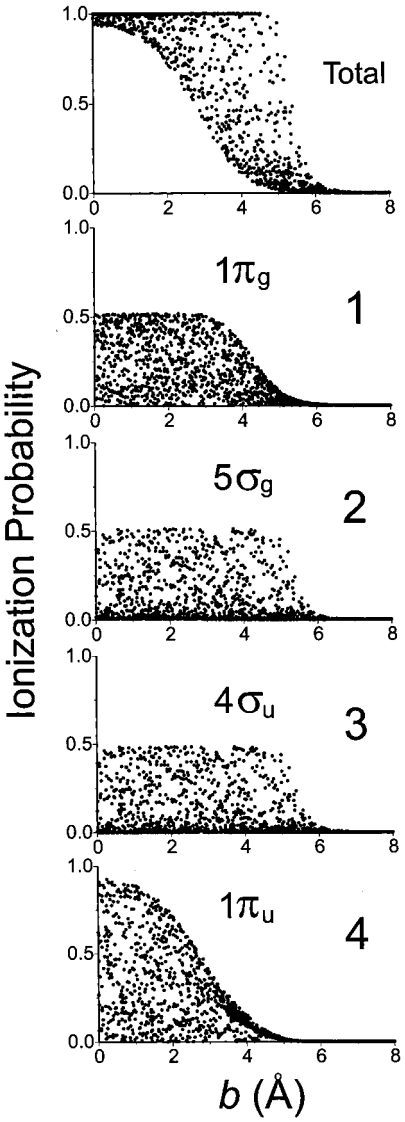

Figure 5. Calculated ionization probabilities as functions of the impact parameter *b* (opacity functions) at the collision energy of 200 meV.

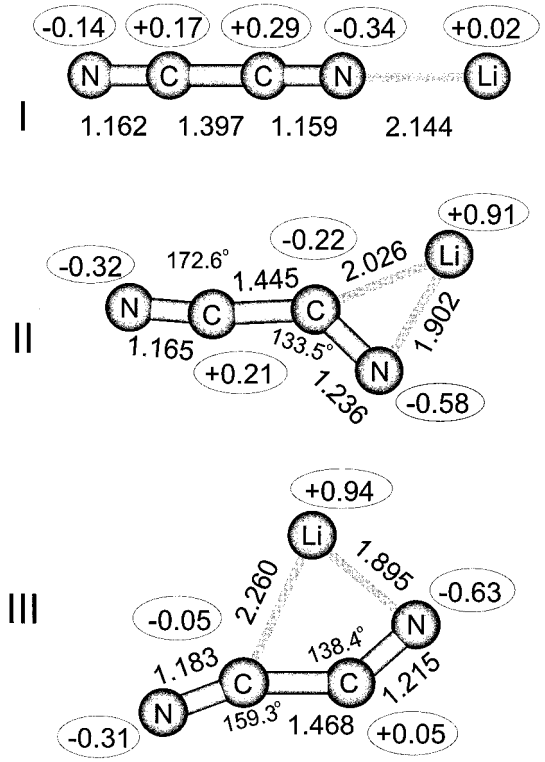

Figure 6. Calculated structure and total atomic charges of NCCNLi radicals (distances in Å).

in the spectrum originate from the removal of an electron from the $1\pi_g$ and $1\pi_u$ orbital, respectively, which can be represented by the out-of-phase and in-phase combination of π_{CN} orbitals. The $1\pi_g$ MO has a nodal surface perpendicular to the molecular frame, going through the symmetry center of the molecule; thus, the highest electron density of $1\pi_g$ is on the CN fragments. $1\pi_u$ is delocalized, but it has the highest electron density in the middle of the molecule, around the C−C bond. The second and third bands in the spectrum originate from the $5\sigma_g$ and $4\sigma_u$ orbitals, respectively, which are the in-phase and out-of-phase combination of the two nitrogen lone pair (or nonbonding) n_N orbitals extending outside to the molecular surface along the σ frame. The localization of $1\pi_g$, $1\pi_u$, and n_N MOs, therefore, provides a possibility to study the anisotropy of the interaction potential around the molecule, using the collision energy dependence of the partial ionization cross sections and peak shifts in the PIES spectrum (see below). The PIES spectrum of NCCN is shown in Figure 1. In the earlier investigation,[13] anomaly in the vibration fine structure of the first band has been observed, which has been explained by a competing autoionization process. We have not observed any unusual fine structure and believe that the anomaly in the previous work is due to the singlet He*(2^1S) atoms in the applied He*(2^1S,2^3S) beam. The observed relative state populations and peak shifts are in good agreement with the earlier investigations. Comparing the UPS and PIES spectra, the relative intensity of n_N bands in the PIES spectrum is strongly enhanced (note that π bands are doubly degenerate). Since metastable atoms cannot penetrate into the interior regions of the molecule, unlike photons, this shows that the n_N MOs are exposed much stronger outside to the molecular surface than π orbitals. There are small peak energy shifts (ΔE_i) in PIES compared to UPS (see Table 1) if the two spectra are compared to each other on an electron energy scale taking the energy of the exciting metastable atom or photon into account. Since the kinetic energy of the ejected electron in Penning ionization depends on the difference between the incoming M + He*(2^3S) (called interaction potential) and outgoing M_i^+ + He potential curves and the outgoing potential can be regarded as flat in the ionization region, the peak shift is determined by the incoming potential. In a simplified sense, one can expect that ΔE_i is positive if the interaction is repulsive and negative if the interaction is attractive. In this latter case, the peak shift is the measure of the well depth of the attractive interaction potential. Negative peak shifts (−70 and −80 meV) were observed on the n_N bands, but no characteristic shift on the π bands. This shows that the interaction between NCCN and He*-(2^3S) is attractive in the nitrogen lone pair region. The shift, however, is surprisingly small compared to the 300−400 meV peak shift of the n_N bands in the spectra of alkyl nitriles,[3,5] as well as the lack of peak shift of π bands; for these latter bands 200−400 meV negative peak shifts were observed in spectra of alkyl derivatives. This indicates that the interaction is much less attractive between NCCN and He*(2^3S) than it is between the −CN group and He*(2^3S) in alkyl nitriles.

Simple theoretical models for describing the collision energy dependence of the ionization cross sections for isotropic atomic targets are well established.[24,35,36] The interaction in this case can be simply described by an interaction potential curve. This simple models, however, can be successfully applied for anisotropic molecular systems as well, where a potential surface

TABLE 1: Band Assignments, Ionization Potentials (IP/eV), Peak Energy Shifts (ΔE/meV), and Slope Parameters (m) for NCCN

		IP/eV					m ($\pm$0.03)[b]	
ionic state	band	expt	HAM3	OVGF[a]	orbital character	ΔE/meV ($\pm$20 meV)	m_1	m_2
$X^2\Pi_g$	1	13.37	13.26	13.35 (0.91)	$1\pi_g(\pi_{CN-})$	+10	−0.08	0.36
$A^2\Sigma_g^+$	2	14.52	14.55	14.58 (0.89)	$5\sigma_g(n_{N+})$	−70	−0.27	0.25
$B^2\Sigma_u^+$	3	14.88	14.99	15.02 (0.87)	$4\sigma_u(n_{N-})$	−80	−0.23	0.31
$C^2\Pi_u$	4	15.60	15.07	15.47 (0.90)	$1\pi_u(\pi_{CN+})$	−10	+0.04	0.25

[a] Pole strength in parentheses. [b] m_1 and m_2 are the slope parameters of the linear fit to the experimental values in the 100−160 meV and 160−300 meV collision energy region, respectively.

TABLE 2: Calculated Vibrational Frequencies (cm^{-1}), IR Intensities (km/mol), Rotational Constants (GHz), Dipole Moments (Debye), Total Energies (au), and Bonding Energies (kJ/mol) of NCCNLi Isomers[a]

NCCNLi (I)		NCCNLi (II)		NCCNLi (III)	
freq	IR int	freq	IR int	freq	IR int
2449 ν_1(CN str)	16.1	2341 ν_1(CN str)	16.8	2124 ν_1(CN s str)	24.4
2238 ν_2(CN str)	1.1	1818 ν_2(CN str)	10.1	1881 ν_2(CN as str)	318.8
868 ν_3(C−C str)	1.9	868 ν_3(C−C str)	2.5	692 ν_3(C−C str)	6.0
530 ν_5(NCCN s def)	37.6	610 ν_4(Li−(CN) str)	150.5	596 ν_4(Li−(CCN) str)	111.2
279 ν_4(Li−N str)	28.5	575 ν_5(NCCN in-plane def)	9.4	531 ν_5(NCCN in-plane def)	10.6
255 ν_6(NCCN as def)	19.4	426 ν_8(out-of-plane def)	24.5	388 ν_8(out-of-plane def)	3.8
112 ν_7(Li−NC def)	7.4	329 ν_6(in-plane def)	26.5	275 ν_6(in-plane def)	45.8
		178 ν_9(out-of-plane def)	3.3	195 ν_9(out-of-plane def.)	19.4
		167 ν_7(in-plane def)	29.3	83 ν_7(in-plane def)	61.9
		$A^b = 37.1543$		$A^b = 24.5547$	
$B^b = 2.4356$		$B = 3.5498$		$B = 4.5008$	
		$C = 3.2402$		$C = 3.8036$	
$\mu^c = 4.81$ (5.21)		$\mu^c = 8.22$ (8.58)		$\mu^c = 5.92$ (5.78)	
total energy = −192.661412		total energy = −192.686634		total energy = −192.675177	
bonding energy[d] = 12.7		bonding energy[d] = 78.9		bonding energy[d] = 48.8	

[a] Calculated at the QCISD/6-311++G** level of theory. [b] Isotopes: C-12, N-14, Li-7. [c] Population analysis was done using the QCISD (SCF) density. [d] Difference between the total energy of the complex and the sum of the energies of fragments.

describes the interaction (in practice several cuts of the potential surface, thus a series of potential curves are used), if there are no irregularities in the simple potential curves describing the gradually changing potential around the target. The negative peak shift in PIES spectrum in this case reflects an average well depth according to the localization of the corresponding MO. According to this theory (see details in the original papers), the collision energy dependence of the ionization cross section can be described by eqs 5 and 6 if the long-range attractive part or the repulsive part of the interaction potential governs the collision energy dependence, respectively (where C, s, b, and d are constants).

$$\sigma(E_c) \propto E_c^{-2/s} \tag{5}$$

$$\sigma(E_c) \propto (\ln E_c/C)^2 (E_c/C)^{b/d-1/2} \tag{6}$$

When the minor collision energy dependence of the first factor ($\ln E_c/C$) is neglected, there is a linear relationship between the collision energy and the ionization cross section on a logarithmic scale ($\log \sigma = m \log E_c + z$, z is a constant). The slope parameter m is negative if the interaction is attractive (see eq 5) and positive if the interaction is repulsive (eq 6), and its absolute value is larger if the interaction is stronger. This linear relationship is widely observed on various molecular targets, which gives reliability to the theory.

The 2D-PIES spectrum, the collision energy dependence of the total and partial ionization cross sections, and the calculated M−Li model potential curves are shown in Figures 2−4. From Figure 3 it is clear that there is no linear relationship between $\log \sigma$ and $\log E_c$ and the collision energy dependence of the total and partial ionization cross section is quite unusual. There is negative collision energy dependence of the ionization cross sections in the 100−160 meV collision energy region, and it is positive between 160 and 300 meV. Thus, there is an unusual change at 160 meV, which indicates an unusual interaction potential surface. Indeed, as we can see in Figure 4, the interaction potential curves at Li−X−N angle of 45°, 60°, and 75° show changing interaction (from repulsive to attractive) due to a second minimum on the potential surface. The calculated ca. 200 meV barrier to this minimum is in good qualitative agreement with the experimentally observed unusual change at 160 meV. In the 100−160 meV collision energy region (and the 100−200 meV on the calculated M−Li curves), there is a linear relationship between $\log \sigma$ and $\log E_c$ (slope parameters m_1 are shown in Table 1). The largest negative collision energy dependence is observed on the n_N bands ($m_1 = -0.27$ and -0.23), a small negative collision energy dependence on the π_g band ($m_1 = -0.08$), and a small positive collision energy dependence on the π_u band ($m_1 = +0.04$). This indicates that the interaction is attractive in the nitrogen lone pair region and gradually changes into small repulsive as the Li−X−N angle opens up from 0° to 90°. This is in good agreement with the calculated M−Li potentials in Figure 4 showing the same trend. The figure also shows that there are trajectories which can lead to the second minimum on the potential surface above 200 meV collision energy, and the number of these trajectories is gradually increasing by increasing the collision energy, because the range of the Li−X−N angle, where Li atoms can get to the second minimum, gradually increases. Since more and more effective trajectory can lead into the region where the ionization probability is higher due to the closer molecular contact, this may explain why the ionization cross section increases in the 160−300 meV region by increasing the collision energy, despite attractive interaction.

For a comparison of the character of the interaction around the parent pseudohalogen NCCN and alkyl-substituted deriva-

tives (R−CN) with He*(2^3S), the collision energy dependence in the 100−160 meV region can be used. The negative collision energy dependence is much smaller in the case of NCCN compared to that of R−CN (the slope parameter for the n_N band is between −0.4 and −0.6, and for the π_{CN} band it is between −0.25 and −0.45),[3,5] indicating a much weaker attractive interaction, which, in good agreement with the peak shifts above, indicates that the electron density on the −CN group in NCCN is smaller than that in R−CN. Regarding the well-known electron-donating effect (+I and +M) of alkyl groups and the large electron negativity of the cyano group, it is not surprising, and it represents a good example of substituent effects.

Classical Trajectory Calculations for Penning Ionization Cross Sections. To eliminate the unusual behavior of the observed collision energy dependence of the ionization cross sections on a quantitative basis and to test the performance of our new method, we have performed theoretical calculations. The theoretical description of the Penning ionization can be divided into two steps: the first is the calculation of the potential energy of the entrance He*−M resonance state, and the second is the calculation of the collision dynamics on the basis of this complex potential. The potential energy of the resonance state can be described in terms of a local complex potential of $V = V_0 - (i/2)\Gamma$, where the real part V_0 is the He*−M interaction potential and the imaginary part Γ is the ionization width for the decay of the He*−M resonance state. In our novel method, ab initio methods are used to calculate V_0 and Γ and classical trajectory calculations to calculate the collision dynamics using the following approximations.

(1) Due to the similarity of the He*−M and Li−M interaction potentials, the real part of the complex potential V_0 is approximated by the computationally more feasible Li−M potential V_0^{Li}.

(2) Neglecting the angular distribution of the ionized electrons, replacing the distance between electrons in two-electron integrals with an average length, and taking into account that the continuum orbitals and helium 2s orbitals are too diffuse compared to the helium 1s and ionized orbitals, thus the positional dependence of the ionization width is governed by the more compact 1s and ionized orbitals, the ionization width for each ionic state is given by

$$\Gamma^{(i)} = K|\langle\Phi_i|\Psi_{1s}\rangle|^2 \qquad (7)$$

where K is a constant and Φ_i and Ψ_{1s} are the ionized molecular orbital and helium atom 1s orbital, respectively.

(3) The molecules are treated as rigid rotators in the classical trajectory calculations.

The theory and approximations are thus well established, and the only limitation of using pure theory for the calculations is that the K constant in eq 7 is not known and it may be different for each colliding molecular system. The determination of K requires the use of at least one experimentally determined physical parameter. In our previous work on N_2, K constant was determined in an iterative way to reproduce the experimental total ionization cross section at 200 meV collision energy. The total ionization cross section, however, is not known for many molecules, and this is the case for NCCN too. In this work, we considered another way to determine K. Although the total ionization cross section is not determined, the dependence of the total ionization cross section on the collision energy is always measured in 2D-PIES and the calculated value depends on K. This dependence, or more precisely the reproducibility of this dependence by varying K on an iterative way, provides a possibility for determining K constant. In the case of most molecules, there is a linear relationship between log σ and log E_c; thus, in practice, the experimental and calculated slope parameters m can be fitted. We have to note, however, that there is an important difference between reproducing the total ionization cross section and reproducing the slope parameter. There is correlation between the interaction potential and K, and both determine the total ionization cross section, as well as the collision energy dependence. The total ionization cross section strongly depends on K, and the calculated value gradually increases by increasing K; therefore, the experimental value can be reproduced, even if the applied interaction potential is not perfect. The slope parameter, however, strongly depends on the interaction potential, and on K in a smaller extent. If the calculated interaction potential is not attractive enough (this is the usual case; see below), the experimental slope parameter cannot be reproduced, only a best agreement between the experimental and calculated value is expected.

The calculations for NCCN in this work are done by varying K constant on an iterative way to obtain the best agreement between the experimental and calculated collision energy dependence of the total ionization cross section. 2000 trajectories are calculated for each collision energy and the initial parameters for trajectories, such as the orientation of the molecule (molecular and rotational axis), impact parameter (between 0 and 10 Å), and rotational energy (300 K) are randomly generated. The results are shown in Figure 3, and calculated total ionization cross sections are found in note 37. There is a good qualitative agreement between the experimental and calculated collision energy dependence. The calculations show that the ionization of n_N MOs have the largest negative collision energy dependence, the dependence of $1\pi_g$ is close to zero, and it is positive for $1\pi_u$ (see note 38). This trend is in good agreement with the experiment, but the calculated values (the slope parameters in the 100−200 meV region) are regularly less negative or more positive, indicating a less attractive or more repulsive interaction. The unusual collision energy dependence of the partial ionization cross sections, i.e., having a minimum in the 100−300 meV region, is also reproduced on the ionization of $1\pi_g$ and n_N MOs (see inset in Figure 3), but the absolute value of the change is smaller than that of the experimental value. The minimum, not surprisingly, was calculated to be at 200 meV, which is the barrier to the second minimum on the calculated M−Li interaction potential surface. This difference between the experimental and calculated values, as well as the calculated collision energy dependence of the ionization cross section, indicates that the calculated M−Li interaction potential, although able to give a good description of the interaction on a qualitative basis, is less attractive (or more repulsive) than it is expected from the experiment. We note that in the case of all molecules that we are currently studying in our laboratory the same effect is observed on the calculated potentials. Possible explanations might be the insufficient inclusion of electron correlation effects in calculations or small geometry relaxation of the molecule by the approach of the metastable atom. This latter is neglected and the frozen molecule approximation has worked very well in qualitative analysis so far. Definitely the extent of this is not clear at the moment and requires further theoretical and experimental work. Clearly, the relaxation effects becomes more important as the speed of the metastable atom decreases, and neglecting them might cause the calculated collision energy dependence to be more positive than the real value. In our previous work on N_2, the calculated M−Li potential has been empirically pulled down, but the potential of NCCN seems to be too difficult to apply a simple correction. For NCCN, we

expect that the description of the interaction potential in the region of the second minimum is more complicated, where relaxation effects and electron correlation effects are expected to be more important (see the geometry of NCCNLi complexes below). The peak shift of −80 meV on n_N bands is in good agreement with the calculated well of ca. 105 meV on the M−Li interaction potential at Li−X−N angle of 0°, but the barrier to the second minimum and the repulsive character especially in the $1\pi_u$ region seems to be exaggerated by calculations.

Figure 5 shows opacity functions for the total and partial ionization cross sections at the collision energy of 200 meV. As it can be seen in the figure, the ionization probability is high if the impact parameter *b* is smaller than 2 Å, it is gradually decreasing with increasing *b*, and there is no effective trajectory, which can lead to ionization, if *b* larger than 6 Å. The opacity functions of the partial ionization cross sections reflect the localization of MOs. Trajectories with small *b* can effectively lead to the ionization of $1\pi_u$ MO, showing that the highest electron density of this MO is at the central part of the molecule, and for the ionization at $b = 5-6$ Å, the nitrogen lone pairs are responsible, which are extended at the two ends of the molecular frame. The plateau behavior of the n_N opacity functions is the result of the localization of n_N MOs at the two ends of the NCCN frame, and vice versa they show that the electron density of these orbitals in the middle of the molecular frame is negligible. Plateau behavior is not observed for the $1\pi_u$ opacity function, and the plateau behavior of $1\pi_g$ functions shows that the $1\pi_g$ MO has highest electron density on the end atoms of NCCN. The analysis of individual trajectories indicates that the upper and lower boundaries of opacity functions are related to some particular trajectories. The upper boundaries of the two n_N opacity functions, corresponding to $5\sigma_g$ and $4\sigma_u$ MOs, are determined by trajectories leading to the nitrogen lone electron pair region. These trajectories also set the lower boundary (zero) of $1\pi_u$ and $1\pi_g$ functions. Since the two n_N MO is very similar and has the highest electron density in the same molecular region, their opacity functions are very similar (MOs are competing in the ionization), and interestingly the sum of the two ionization probabilities in the upper boundary gives the upper boundary of the opacity function of the total ionization cross section. The upper boundary of $1\pi_u$ opacity function is determined by trajectories leading to the middle of the NCCN frame, and trajectories perpendicular to the frame have the largest ionization probability. These trajectories set the lower boundary of n_N and $1\pi_g$ opacity functions as well. It is interesting to find that the trajectories determining the upper boundary of the $1\pi_u$ opacity function determine the lower boundary of that of the total ionization cross section, and the trajectories determining the upper boundary of n_N opacity functions set the upper boundary of that of the total. Since the localization of $1\pi_u$ and n_N MOs is very different, NCCN is an ideal case where this clear difference between opacity functions and collisional dynamics can be observed. The opacity function of $1\pi_g$ MO is just between the $1\pi_u$ and n_N functions in many respects, in good agreement with the orbital's intermediate localization, having the highest electron density around an N−X−He* angle of 45°. The opacity functions clearly show that there is a high (close to 1) ionization probability for n_N MOs if He* approaches the molecule at a small N−X−He* angle, and this gradually decreases by increasing the N−X−He* angle. The situation for $1\pi_u$ is just the opposite.

NCCNLi Inorganic Radicals. Due to the similarity of M−He*(2^3S) and M−Li(2^2S) interaction potentials, and given that this latter is the ground state potential of the M−Li system, PIES spectroscopy is able to predict the existence of thermodynamically stable MLi radicals. Their existence is expected if the interaction is attractive, and there is a large negative peak shift in the PIES spectrum. The peak shift is a good estimation of the bonding energy of the radical if there is no large geometry relaxation of M by the formation of MLi (due to the fast metastable atom the geometry of M is frozen) and the corresponding MO is localized. PIES investigation and model potentials (see above) indicated that at least two different NCCNLi complexes can form from NCCN and Li. To obtain information about the structure and stability of these complexes, full geometry optimizations have been performed at the QCISD/6-311++G** level. Calculations have found three minima on the potential energy surface, and they are shown in Figure 6. The first complex, NCCNLi(I), has a linear structure, where the NCCN ligand bonds with the nitrogen lone pair to Li with a coordinative bond. The total atomic charge on Li is close to zero (+0.02), and the molecular orbital analysis shows that the lithium unpaired electron stays on Li. The geometry of NCCN does not change significantly compared to the free NCCN molecule. The calculated bonding energy of this complex is 12.7 kJ/mol (= 132 meV), which is in good agreement with the 80 meV negative peak shift of the n_N band in the PIES spectrum. This complex represents the case where the peak shifts in PIES is a good estimation of the stability of the corresponding MLi radical. (Note that in the case of molecular target the well on the potential surface must be somewhat larger than the peak shift depending on the localization of the MO.) The second and third complexes have a different structure, and they can be characterized as π-complexes. The lithium unpaired electron completely delocalizes on the NCCN frame, and as a consequence the charge on Li is close to +1 (see Figure 6). The bonding energy of these complexes is much larger than that of NCCNLi(I). By investigating the formation of MOs of NCCNLi complexes from their NCCN and Li fragments, the same stabilizing effect has been observed that has been found in the case of HNNNLi and HCNOLi in our previous work.[7] As a result of the bending of the NCCN frame, the LUMO of NCCN is stabilized and thus interacts strongly with the LUMO of Li atom, which results in further large stabilization. The delocalization of the Li unpaired electron into this stabilized lower lying MO results in large bonding energy in complexes NCCNLi(II) and NCCNLi(III). This cannot happen in NCCNLi(I); thus the bonding energy is much smaller and the lithium unpaired electron stays on the destabilized Li 2s orbital. The bonding energy of 78.9 kJ/mol (818 meV) and 48.8 kJ/mol (506 meV) for NCCNLi(II) and NCCNLi(III), respectively, also indicates that large geometry relaxation in the Penning ionization cannot happen, because this should cause very large peak shifts on π bands. Since practically no peak shift is observed on these bands, this gives reliability for the frozen molecule approximation in the Penning ionization process in qualitative analysis (see Discussion above).

The formation of π-complexes and their large bonding energy is an interesting result of this work. Our previous study on CH_3-CNLi and $Li_n(CH_3CN)_m$ clusters has indicated that the most stable form of these molecules or clusters is that where the CH_3-CN bonds to Li with the nitrogen lone pair (similarly to NCCNLi(I)).[3,39] The strong tendency of NCCN to form π-complexes with Li may cause interesting complex or cluster behaviors. The identification of NCCNLi isomers is feasible either in inert solid matrix or in the dilute gas phase. To support future identifications, calculated harmonic vibrational frequen-

cies, infrared intensities, rotational constants, and dipole moments are shown in Table 2.

Conclusion

The NCCN molecule can be generated into the gas phase in good yield from solid−solid reaction between rubeanic acid and yellow mercury(II) oxide and by gas-phase thermolysis of mercury(II) cyanide or cyanogen iodide. The molecule is characterized in the gas phase by Penning and He I photoelectron spectroscopies. From spectroscopic investigations, the interaction potential between NCCN and He*(2^3S) atoms is deduced, which is attractive in the nitrogen lone electron pair region and gradually changes into weakly repulsive by going from the end of the NCCN frame into the middle. Model potential calculations on the similarly interacting NCCN−Li(2^2S) system are in good qualitative agreement with experimental results. Furthermore, they provide explanation for the observed unusual collision energy dependence of the ionization cross sections. Classical trajectory calculations have also been performed for the understanding of collision dynamics. They are in qualitative agreement with the experiment, but the quantitative description of the collision energy dependence of the ionization cross sections is fair. The quantitative description of this latter is a difficult but an interesting challenge for future theoretical calculations.

NCCN readily forms complexes with lithium atom, and ab initio calculations identified three isomers: one classical-type complex, where NCCN bonds to Li by one of the nitrogen lone electron pairs, and two π-complexes. These π-complexes are thermodynamically more stable than the classical one, and the large bonding energy is explained by the delocalization of the lithium unpaired electron on the NCCN frame.

Acknowledgment. We thank the Japanese Ministry of Education, Science, and Culture for a Grant in Aid for Scientific Research in support of this work. T.P. thanks the Japan Society for the Promotion of Science (JSPS) for a JSPS Invitation Fellowship (ID No. L98519) and the Hungarian Scientific Research Fund (OTKA Grant F022031) in support of this work.

References and Notes

(1) Ohno, K.; Harada, Y. Penning Ionization−The Outher Shape of Molecules. In *Molecular Spectroscopy, Electronic Structure and Intramolecular Interactions*; Maksic, Z. B., Ed.; Springer-Verlag: New York, 1991.
(2) Ohno, K.; Yamakado, H.; Ogawa, T.; Yamata, T. *J. Chem. Phys.* **1996**, *105*, 7536.
(3) Pasinszki, T; Yamakado, H.; Ohno, K. *J. Phys. Chem.* **1995**, *99*, 14678.
(4) Kishimoto, N.; Yokoi, R.; Yamakado, H.; Ohno, K. *J. Phys. Chem. A* **1997**, *101*, 3284.
(5) Kishimoto, N.; Aizawa, J.; Yamakado, H.; Ohno, K. *J. Phys. Chem. A* **1997**, *101*, 5038.
(6) Ogawa, T.; Ohno, K. *J. Chem. Phys.* **1999**, *110*, 3773.
(7) Pasinszki, T; Kishimoto, N.; Ohno, K. Submitted for publication.
(8) Baker, C.; Turner, D. W. *Proc. R. Soc. A* **1968**, *308*, 19.
(9) Hollas, J. M.; Sutherley, T. A. *Mol. Phys.* **1972**, *24*, 1123.
(10) Åsbrink, L.; von Niessen, W.; Bieri, G. *J. Electron Spectrosc. Relat. Phenom.* **1980**, *21*, 93.
(11) Fridh, C.; Åsbrink, L.; Lindholm, E. *Chem. Phys.* **1978**, *27*, 169.
(12) Čermák, V.; Yencha, A. J. *J. Electron Spectrosc. Relat. Phenom.* **1976**, *8*, 109.
(13) Yee, D. S. C.; Brion, C. E. *J. Electron Spectrosc. Relat. Phenom.* **1976**, *8*, 313.
(14) Pasinszki, T.; Westwood, N. P. C. *J. Phys. Chem.* **1995**, *99*, 1649.
(15) *Gmelins Handbuch der anorganischen Chemie*; Verlag Chemie GMBH: Weinheim, 1971; Kohlenstoff, Teil D 1, p 85.
(16) Gay-Lussac, L. J. *Ann. Chim. (Paris)* **1815**, *95*, 175.
(17) Lewis, G. N.; Keyes, D. B. *J. Am. Chem. Soc.* **1918**, *40*, 472.
(18) Takami, T.; Mitsuke, K.; Ohno, K. *J. Chem. Phys.* **1991**, *95*, 918.
(19) Takami, T.; Ohno, K. *J. Chem. Phys.* **1992**, *96*, 6523.
(20) Mitsuke, K.; Takami, T.; Ohno, K. *J. Chem. Phys.* **1989**, *91*, 1618.
(21) Gardner, J. L.; Samson, J. A. R. *J. Electron Spectrosc. Relat. Phenom.* **1976**, *8*, 469.
(22) Kimura, K.; Katsumata, S.; Achiba, Y.; Yamazaki, T.; Iwata, S. *Handbook of He I Photoelectron Spectra of Fundamental Organic Molecules*; Japan Scientific Press: Tokyo, 1981.
(23) (a) Rothe, E. W.; Neynaber, R. H.; Trajillo, S. M. *J. Chem. Phys.* **1965**, *42*, 3310. (b) Hotop, H. *Radiat. Res.* **1974**, *59*, 379. (c) Haberland, H.; Lee, Y. T.; Siska, P. E. *Adv. Chem. Phys.* **1981**, *45*, 487.
(24) Niehaus, A. *Adv. Chem. Phys.* **1981**, *45*, 399.
(25) Maki, A. G. *J. Chem. Phys.* **1965**, *43*, 3193.
(26) Boys, S. F.; Bernardi, F. *Mol. Phys.* **1970**, *10*, 553.
(27) Frisch, M. J.; Trucks, G. W.; Schlegel, H. B.; Gill, P. M. W.; Johnson, B. G.; Robb, M. A.; Cheeseman, J. R.; Keith, T.; Petersson, G. A.; Montgomery, J. A.; Raghavachari, K.; Al-Laham, M. A.; Zakrzewski, V. G.; Ortiz, J. V.; Foresman, J. B.;Cioslowski, J.; Stefanov, B. B.; Nanayakkara, A.; Challacombe, M.; Peng, C. Y.; Ayala, P. Y.; Chen, W.; Wong, M. W.; Andres, J. L.; Replogle, E. S.; Gomperts, R.; Martin, R. L.; Fox, D. J.; Binkley, J. S.; Defrees, D. J.; Baker, J.; Stewart, J. P.; Head-Gordon, M.; Gonzalez, C.; Pople, J. A. *Gaussian 94*, revision C.3; Gaussian, Inc.: Pittsburgh PA, 1995.
(28) von Niessen, W.; Schirmer, J.; Cederbaum, L. S. *Comput. Phys. Rep.* **1984**, *1*, 57.
(29) Åsbrink, L.; Fridh, C.; Lindholm, E. *Chem. Phys. Lett.* **1977**, *52*, 69. The HAM/3 program is available from the Quantum Chemistry Program Exchange, Indiana University, Bloomington, IN (D. P. Chong, QCMP005, 1985).
(30) Chong, D. P. *Theor. Chim. Acta.* **1979**, *51*, 55.
(31) von Niessen, W.; Cederbaum. L. S.; Schirmer, J.; Diercksen, G. H. F.; Kraemer, W. P. *J. Electron Spectrosc. Relat. Phenom.* **1982**, *28*, 45.
(32) Scheller, M. K.; Weikert, H. G.; Cederbaum, L. S.; Tarantelli, F. *J. Electron Spectrosc. Relat. Phenom.* **1990**, *51*, 75.
(33) Cederbaum, L. S.; Domcke, W.; Schirmer, J.; Köppel, H. *J. Chem. Phys.* **1980**, *72*, 1348.
(34) Decleva, P.; Lisini, A. *Chem. Phys.* **1987**, *112*, 339.
(35) Illenberger, E.; Neihaus, A. *Z. Phys. B* **1975**, *20*, 33.
(36) Allison, W.; Muschlitz, E. E., Jr. *J. Electron Spectrosc. Relat. Phenom.* **1981**, *23*, 339.
(37) Calculated total Penning ionization cross sections for NCCN at 100, 200, 300, 400, and 500 meV collision energy, respectively, are 53.94, 54.93, 56.71, 57.43, and 57.96 Å^2.
(38) Calculated slope parameters (fitted to the calculated partial ionization cross sections between 100 and 200 meV; m_1) for the ionization of $1\pi_g$, $5\sigma_g$, $4\sigma_u$, and $1\pi_u$ MOs, respectively: +0.01, −0.14, −0.16, and +0.34.
(39) Ohshimo, K.; Tsunoyama, H.; Yamakita, Y.; Misaizu, F.; Ohno, K. *Chem. Phys. Lett.* **1999**, *301*, 356.